Virus-induced gene silencing in the perennial woody *Paeonia ostii*

Lihang Xie [Equal first author, 1], **Qingyu Zhang** [Equal first author, 1], **Daoyang Sun** [1], **Weizong Yang** [1], **Jiayuan Hu** [1], **Lixin Niu** [Corresp., 1], **Yanlong Zhang** [Corresp. 1]

[1] College of Landscape Architecture and Arts, Northwest A&F University, Yangling, Shaanxi, China

Corresponding Authors: Lixin Niu, Yanlong Zhang
Email address: niulixin@nwafu.edu.cn, zhangyanlong@nwafu.edu.cn

Tree peony is a perennial deciduous shrub with great ornamental and medicinal values. A limitation for its current functional genomic research is the lack of effective molecular genetic tools. Here, the first application of a *Tobacco rattle virus* (TRV)-based virus-induced gene silencing (VIGS) in the tree peony species *Paeonia ostii* is presented. Two different approaches, leaf syringe-infiltration and seedling vacuum-infiltration, were utilized for *Agrobacterium*-mediated inoculation. The vacuum-infiltration was shown to result in a more complete *Agrobacterium* penetration than syringe-infiltration, and thereby determined as an appropriate inoculation method. The silencing of reporter gene *PoPDS* encoding phytoene desaturase was achieved in TRV-*PoPDS*-infected triennial tree peony plantlets, with a typical photobleaching phenotype shown in uppermost newly-sprouted leaves. The endogenous *PoPDS* transcripts were remarkably down-regulated in VIGS photobleached leaves. Moreover, the green fluorescent protein (GFP) fluorescence was detected in leaves and roots of plants inoculated with TRV-GFP, suggesting the capability of TRV to silence genes in various tissues. Taken together, the data demonstrated that the TRV-based VIGS technique could be adapted for high-throughput functional characterization of genes in tree peony.

Virus-induced gene silencing in the perennial woody *Paeonia ostii*

Lihang Xie† · Qingyu Zhang† · Daoyang Sun† · Weizong Yang · Jiayuan Hu · Lixin Niu* · Yanlong Zhang*

College of Landscape Architecture and Arts, Northwest A&F University, Yangling, Shaanxi 712100, People's Republic of China; Oil Peony Engineering Technology Research Center of National Forestry Administration, Yangling, Shaanxi, People's Republic of China

* To whom correspondence should be addressed:

Lixin Niu

College of Landscape Architecture and Arts, Northwest A&F University, Yangling, Shaanxi, People's Republic of China

Tel: +86-13572582039; Fax: +86-029-87082878; E-mail: niulixin@nwsuaf.edu.cn

Yanlong Zhang

College of Landscape Architecture and Arts, Northwest A&F University, Yangling, Shaanxi, People's Republic of China

Tel: +86-029-87082878; Fax: +86-029-87082878; E-mail: zhangyanlong@nwsuaf.edu.cn

† These authors contributed equally to this work.

Abstract

Tree peony is a perennial deciduous shrub with great ornamental and medicinal values. A limitation for its current functional genomic research is the lack of effective molecular genetic tools. Here, the first application of a *Tobacco rattle virus* (TRV)-based virus-induced gene silencing (VIGS) in the tree peony species *Paeonia ostii* is presented. Two different approaches, leaf syringe-infiltration and seedling vacuum-infiltration, were utilized for *Agrobacterium*-mediated inoculation. The vacuum-infiltration was shown to result in a more complete *Agrobacterium* penetration than syringe-infiltration, and thereby determined as an appropriate inoculation method. The silencing of reporter gene *PoPDS* encoding phytoene desaturase was achieved in TRV-*PoPDS*-infected triennial tree peony plantlets, with a typical photobleaching phenotype shown in uppermost newly-sprouted leaves. The endogenous *PoPDS* transcripts were remarkably down-regulated in VIGS photobleached leaves. Moreover, the green fluorescent protein (GFP) fluorescence was detected in leaves and roots of plants inoculated with TRV-GFP, suggesting the capability of TRV to silence genes in various tissues. Taken together, the data demonstrated that the TRV-based VIGS technique could be adapted for high-throughput functional characterization of genes in tree peony.

Abbreviations

TRV	*Tobacco rattle virus*
VIGS	Virus-induced gene silencing
PTGS	Post-transcriptional gene silencing
PDS	Phytoene desaturase
EGFP	Enhanced green fluorescent protein
qRT-PCR	Quantitative real-time PCR

Introduction

Tree peony is a perennial woody plant belonging to sect. *Moutan* DC. of the genus *Paeonia* L. (Paeoniaceae) (*Li et al., 2009*). It is indigenous to China and the cultivation history can be traced back to 2000 years ago (*Chen & Li, 1998*). As China's unofficial national flower, tree peony has been introduced to Japan, America, Australia, and Europe, with a rise in worldwide popularity. It is commonly known as an ornamental and medicinal crop due to large showy flowers and abundant bioactive substances in roots. Recent reports suggest that the tree peony seed has high yield of oil which contains over 90% unsaturated fatty acids required by human, revealing a tremendous potential of tree peony in future edible oil production (*Wu et al., 2014*). The variety *Paeonia ostii* 'Feng Dan' (*P. ostii* 'Feng Dan') is a new oil crop widely planted in north China,

63 with its total cultivated area exceeding 16,200 hectares.

64 For now, a quantity of studies have been carried out on the cloning and function analysis of
65 genes, associated with flower development (*Li et al., 2016*), bud dormancy (*Zhang et al., 2015b*),
66 anthocyanin accumulation (*Zhang et al., 2015a*), and fatty acid biosynthesis (*Yin et al., 2018*), in
67 tree peony. However, the conclusive studies on the function of genes in tree peony are tough
68 because the lack of efficient genetic transformation system. Besides, the transgenic technology is
69 time-consuming and laborious for the generation of homozygous lines, especially for plants with
70 long life cycle like tree peony.

71 Virus-induced gene silencing (VIGS) is an attractively quick strategy for reverse genetic
72 manipulation of non-model plants bypassing the stable transformation process (*Ruiz et al., 1998*;
73 *Burch-Smith et al. 2004*). The VIGS experiment relies on the recombinant virus vector carrying
74 an inserted partial sequence of a target plant gene to initiate RNA-mediated post-transcriptional
75 gene silencing (PTGS), leading to transcript suppression of corresponding homologous gene
76 (*Baulcombe, 1999*; *Burch-Smith et al., 2004*; *Dinesh-Kumar et al., 2011*). In this mechanism,
77 double-stranded chimeric intermediates are first formed during viral replication in plant. Theses
78 foreign intermediate are recognized and cleaved into 21-23 nucleotides of short interfering RNAs
79 (siRNAs) by the enzyme DICER. Next, siRNAs are incorporated into the RNA-induced
80 silencing complex (RISC) and target the complementary transcripts for cleavage, thus resulting
81 in a specific degradation of host mRNA (*Bartel, 2004*; *Senthil-Kumar & Mysore, 2011*). In
82 contrast to gene silencing methods with inverted repeat sequences, VIGS has several advantages
83 as simple plasmid assembly, short implementation cycle, and available identification of embryo-

lethal genes (*Reid et al., 2009*).

Many viral vectors have been developed for VIGS assay, including *Apple latent spherical virus* (ALSV), *Barely stripe mosaic virus* (BSMV) (*Holzberg et al., 2002*), *Cucumber mosaic virus* (CMV) (*Tasaki et al., 2016*), *Potato virus X* (PVX) (*Faivrerampant et al., 2004*), *Tobacco mosaic virus* (TMV) (*Kumagai et al., 1995*), and *Tobacco rattle virus* (TRV) (*Ratcliff et al., 2001*). Compared to other viruses, TRV is capable of reaching apical meristem, inducing mild symptoms, and infecting wide range of plant species. Consequently, TRV vector has been widely used for silencing genes in a number of eudicots and monocots (*Purkayastha & Dasgupta, 2009*), such as Arabidopsis (*Burchsmith et al., 2006*), tobacco (*Liu et al., 2002*), tomato (*Quadrana et al., 2011*), petunia (*Sun et al., 2017*), strawberry (*Jia et al., 2011*), rose (*Wu et al., 2016*), gladiolus (*Singh et al., 2013*), wheat, and maize (*Zhang et al., 2017*). At present, the VIGS technique is mostly applied to small herbaceous plants, and only a minority of woody plants achieves the set-up of VIGS system, like physic nut (*Ye et al., 2009*), grape (*Kurth et al., 2012*), and apple (*Yamagishi & Yoshikawa, 2013*). The previous evidences indicate that tobacco rattle virus has been found in peony (*Paeonia lactiflora* 'Sarah Bernhardt') (*Robertson et al. 2009*). However, whether TRV-based VIGS can be applied to tree peony remains largely unknown.

Reporter gene is an essential component for indicating sites of silencing in VIGS system. PHYTOENE DESATURASE (PDS) is a key enzyme in the biosynthesis of protective carotene (*Cunningham & Gantt, 1998*). Silencing of *PDS* results in characteristic photobleaching symptoms in infected plants (*Stilio et al., 2010*), and therefore it usually serves as a clear reporter. A modified TRV-GFP vector, bearing the coding region of enhanced green fluorescence protein

(EGFP), also provides a visual tool for monitoring virus spread and silencing efficiency. This vector has been successfully tested in several plants, including Arabidopsis, tobacco, rose, strawberry, and chrysanthemum (*Tian et al., 2014*). In this study, we established an effective VIGS system in *P. ostii* triennial seedlings by vacuum infiltration of TRV-*PoPDS* and TRV-GFP. The upper systemically-infected leaves with TRV-*PoPDS* displayed a prominent photobleaching phenotype and decreased *PoPDS* transcripts. GFP fluorescence was observed in TRV-GFP-infiltrated leaves and roots under UV light irradiation. The data we have obtained demonstrated the value of TRV-based VIGS for unraveling the functional significance of genes in tree peony.

Materials and Methods

Plant materials and growth conditions

Three-year-old seedlings of tree peony (*P. ostii* 'Feng Dan') at four weeks post germination were used for VIGS assay (Fig. 1a). The whole plant and leaves were agro-infiltrated with disposable syringe and vacuum pressure for infection of TRV constructs, respectively. After inoculation, the tree peony seedlings were rinsed with distilled water once and planted into plastic pots containing a mixture of peat moss and vermiculite in a 3:1 volume ratio. Those plants were first kept in the dark room at 15 ℃ for one week, and then transferred into a growth chamber with a 16 h light/ 8 h dark photoperiod, and a day/night temperature range of 20/18 ℃. The inoculated and uppermost systemically-infected leaves were used for phenotype observation, expression profile analysis, and GFP fluorescence detection.

126 **Isolation and sequence analysis of *PoPDS***

127 Total RNA was extracted from the *P. ostii* 'Feng Dan' leaves with the TIANGEN RNA Prep
128 Pure Plat kit according to the manufacturer's recommendations (Tiangen, China). The first strand
129 of cDNA was synthesized using PrimeScript® RT reagent Kit with gDNA Eraser (Takara, Japan).
130 Primers were designed to amplify the *PoPDS* coding sequence based on transcriptome data
131 during leaf development of *P. suffruticosa* Andrews (*Luo et al., 2017*). PCR was conducted using
132 Taq DNA polymerase (Invitrogen, USA). The PCR reaction procedure was as follows: a cycle of
133 94 ℃ for 5 min; 35 cycles of 94 ℃, 30 s, 54 ℃, 30 s, 72 ℃, 30 s; a final cycle of 72 ℃ for 10
134 min. Next, the PCR products were cloned into the pUCm-T vector (TaKaRa, Japan). Positive
135 clones were confirmed by DNA sequencing. Corresponding amino acids were deduced through
136 the ExPASy translate tool (http://web.expasy.org/translate/). Multiple sequence alignment of
137 PoPDS with other similar proteins was performed by CLUSTALW
138 (http://www.genome.jp/tools/clustalw/).
139
140 **Plasmid construction**
141 The TRV1, TRV2, and TRV2-GFP plasmids were kindly provided by Dr. Yule Liu (Tsinghua
142 University, China). To generate the TRV-*PoPDS* construct, a 195-bp *PoPDS* fragment was PCR-
143 amplified using specific primers (Table 1), and cloned into the pUCm-T vector by T4 DNA
144 ligase (Sangon, China). This recombinant plasmid was digested with *Bam*HI and *Eco*RI
145 restriction enzymes, and the fragment of *PoPDS* (GenBank accession number: MK733916) was
146 ligated into corresponding sites of TRV2 vector (Fig. S2). The resulting construct was then

147 transformed into *Eacherichia coli* strain DH5α competent cells, which were selected on LB
148 plates containing 50 mg l^{-1} of kanamycin. PCR was used to examine the presence of *PoPDS*
149 insert in the generated construct.
150
151 **Agro-inoculation of TRV vector**
152 TRV1, TRV2, and its derivatives were introduced into *Agrobacterium tumefaciens* strain
153 GV3101 via freeze-thaw method (*Yan et al., 2012*). The transformed bacteria bearing TRV
154 constructs were cultured in LB medium supplemented with 40 mg l^{-1} kanamycin, 20 mg l^{-1}
155 gentamicin, 10 mM MES, and 20 μM acetosyringone at 28 ℃ in a growth chamber for 48 h.
156 *Agrobacterium* cultures were centrifuged at 4000 *g* for 20 min, and resuspended in the
157 infiltration buffer (10 mM $MgCl_2$, 10 mM MES, and 200 μM acetosyringone) to a final OD_{600} of
158 1.0. The cultures containing TRV1 and TRV2 constructs was shaken gently for 4-6 h at room
159 temperature and mixed together in a 1:1 ratio before inoculation. For syringe infiltration, the
160 abaxial sides of two or three fully expanded leaves were injected using a 1-ml needleless syringe.
161 For vacuum infiltration, the whole plants were submerged in the infiltration buffer and subjected
162 to 0.1 MPa vacuum pressure for 20 min. Approximately 50 tree peony seedlings were inoculated
163 by vacuum method for each assay.
164
165 **Semi-quantitative RT-PCR and quantitative real-time PCR**
166 Total RNA was extracted from inoculated and systemically-infected leaves of tree peony
167 seedlings, and purified with RNase-free DNase (Takara, Japan). First-strand cDNA as the

168 template for PCR was synthesized from 2-5 μg of total RNA. Three primer pairs were designed
169 to detect the presence of TRV (Table 1). Since the forward and reverse primers of TRV2-2
170 covered the multiple cloning sites (MCS), the size of resulting product varied depending on the
171 inserts in the site, whereas the TRV1 and TRV2-1 primers led to the bands with the same sizes
172 (*Sun et al., 2016*). The PCR products were analyzed through electrophoresis using a Molecular
173 Imager Gel Doc XR+ System (Bio-Rad, USA). Quantitative real-time PCR (qRT-PCR) was
174 carried out using SYBR Premix Ex Taq II (Takara, Japan) in a 20-μl PCR mixture and analyzed
175 by a StepOnePlus Real-time PCR System (Applied Biosystems, USA). 18S-26S internal
176 transcribed spacer was used as an internal control to normalize the expression data (*Zhang et al.,*
177 *2018*). The PCR primers, used for the determination of transcript abundances of *PoPDS*, were
178 designed outside the region of the inserted fragment to avoid amplification of the fragment
179 included in TRV2 construct.
180
181 **GFP imaging**
182 Transient assay of GFP in the inoculated leaf and root cells of *P. ostii* was conducted based on
183 the agro-infiltration with TRV-GFP. GFP fluorescence was detected and photographed using a
184 laser scanning confocal microscope (Leica TCS SP8).
185
186 **Western blot**
187 A GFP-specific antibody (Abcam Inc) was used to implement western blot analysis. Proteins
188 were extracted from leaves and roots of *P. ostii* plants, with 300 μL extraction buffer (100 mM

189 Tris pH=6.8, 2.5% SDS, 100 mM dithiothreitol, 100 mM NaCl, and 10% glycerol). Bradford
190 assay was used to determine protein quantities, and equal amounts of proteins for each sample
191 were separated by 10% SDS-PAGE (*Bradford, 1976*). Next, proteins were transferred to a
192 polyvinylidene difluoride membrane (GE healthcare). CP-GFP was detected after an overnight
193 incubation at room temperature with a 1:10,000 dilution of the anti-GFP antibody conjugated to
194 alkaline phosphatase (*Tian et al., 2014*). Alkaline phosphatase was detected using a
195 chemiluminescent substrate (CSPD; Roche) and exposed to X-ray film (Kodak X-OMAT BT
196 Film/XBT-1).
197
198 **Results**
199 **Comparison of the agro-infiltration methods**
200 In view of the woody characteristics of tree peony, choosing a plant with optimal age and size for
201 VIGS assay is pre-requisite. Three-year-old young plantlets were therefore used because of their
202 delicate underground roots, small plant type, and high occurrence of new leaves (Fig. 1a). To
203 determine the most appropriate method of *Agrobacterium*-mediated TRV infection in tree peony,
204 leaf syringe-infiltration and seedling vacuum-infiltration were selected for comparison (Fig. 1b).
205 We found that the vacuum infiltration brought about a more sufficient permeation of bacterial
206 cultures through the abaxial leaf surface than the syringe infiltration, which made the infiltration
207 happen only at the inoculation sites. Furthermore, the syringe infiltration inevitably caused
208 obvious mechanical damage to leaf tissues (Fig. 1c). Semi-quantitative RT-PCR analysis
209 indicated that TRV1 and TRV2 transcripts were detected in all inoculated leaves by both

infiltration methods, but not in untreated leaves (Fig. 1d). And, the TRV transcripts accumulation levels in vacuum-infiltrated leaves are obviously higher than that in syringe-infiltrated leaves. According to the results, vacuum infiltration was used for subsequent gene-silencing experiments.

Identification of *PoPDS*

Phytoene desaturase (*PDS*) is commonly used as a visible reporter for silencing. Based on the transcriptome data obtained from developing leaves of tree peony, we PCR-amplified the open reading frame (ORF) nucleotide sequence of *P. ostii PDS*, annotated as *PoPDS*. *PoPDS* was predicted to encode a protein of 575 amino acids, and conserved domain analysis revealed a putative dinucleotide binding domain in its deduced protein sequence. Multiple sequence alignments showed that amino acid sequence of *PoPDS* shared high similarity with the homologies from other plant species, such as *Vitis vinifera*, *Nicotiana tabacum*, *Arabidopsis thaliana*, and *Petunia hybrida* (Fig. S2). The full-length amino acid sequence of PoPDS had 83.3%, 82.09%, 79.96%, and 80.7% identities with those of four plant species, respectively.

Silencing of *PoPDS* in *P. ostii* leaves

To assess the feasibility of TRV-based VIGS in tree peony, we introduced a 195-bp conserved fragment of *PoPDS* into TRV2 vector, and generated a TRV-*PoPDS* recombinant (Fig. 2). Upon *Agrobacterium*-mediated infection, similar necrotic symptoms occurred in the edge of leaves infiltrated with TRV empty vector and TRV-*PoPDS*, while the remaining area seems normal (Fig. 3a). Approximately 52% of seedlings exhibited a remarkable photobleaching phenotype in

231 the first newly developed leaves at 4 weeks post inoculation. White spots or sectors were clearly
232 observed throughout the upper leaves particularly around leaf main veins. This phenotype
233 remained stable and persisted for about 2 months under growth chamber conditions (Fig. S3).

234 To confirm the correlation of leaf photobleaching with the presence of the viral vectors, TRV
235 accumulation was examined using semi-quantitative RT-PCR. TRV1 and TRV2 were detected in
236 TRV empty vector- and TRV-*PoPDS*-infected leaves, but not in the mock control plants (Fig.
237 3b). When using primers covering MCS of TRV2 vector, a fragment carrying *PoPDS* insert was
238 detected in the leaves agro-infiltrated with TRV-*PoPDS*. 18S-26S internal transcribed spacer was
239 referred as an internal control for normalization of gene expression. QRT-PCR analysis
240 demonstrated that transcript abundances of *PoPDS* were significantly reduced in photobleached
241 leaves of plants infiltrated with TRV-*PoPDS*, compared with that in mock- and TRV empty
242 vector-inoculated seedlings (Fig. 3c). These results suggested that the leaf photobleaching
243 phenotype was initiated by *PoPDS* silencing. It indicated that the *PoPDS* of tree peony could be
244 silenced by VIGS and TRV infection was systemically established.

245

246 **Validation of TRV-GFP in *P. ostii* leaves and roots**

247 Apart from TRV-*PoPDS*, another visualizable vector TRV-GFP, in which the EGFP coding
248 sequence was fused to coat protein ORF of TRV2, was used for infiltration to monitor virus
249 spread in *P. ostii*. Under a confocal microscope, GFP fluorescence was observed in the newly
250 emerging leaves and roots of plants at 5 days post inoculation (dpi) with TRV-GFP, indicating
251 the capability of TRV vector to express foreign genes in different tree peony tissues. No

252 fluorescence signals were detected in mock control leaves and roots (Fig. 4).

253 Moreover, we performed western blot analysis to check the expression of GFP protein in
254 infected leaves and roots. As illustrated in Fig. 5a, GFP proteins were accumulated in the leaves
255 and roots of plants inoculated with TRV-GFP, whereas no GFP bands were found in control
256 plants. By contrast, the GFP abundances in infected roots appeared to be much higher than that
257 in infected leaves (Fig. 5a). Semi-quantitative RT-PCR analysis revealed a consistent variance
258 that the roots exhibited more transcripts of TRV1, TRV2, and GFP than the leaves (Fig. 5b). The
259 data suggested that the systemic movement of TRV vector in tree peony plants could be
260 effectively supervised via the GFP-tagged expression.

261

262 **Discussion**

263 In addition to the significance floral characteristics of tree peony, its roots contains some special
264 secondary metabolites, which are generally used as traditional Chinese medical materials, and its
265 leaves also has excellent ornamental values owing to its changeable color during the early
266 growth period (*Luo et al., 2017*; *Li et al., 2018*). Therefore, there are considerable interests in
267 evaluating the gene function in both roots and leaves of tree peony. However, an effective
268 genetic transformation system is still unavailable in tree peony because of severe callus
269 browning and tough plant regeneration (*Liu & Jia, 2010*). Few studies on molecular functional
270 identification have been performed in tree peony due to this limitation. It seems likely that a
271 transient expression system for up- or -down-regulation of genes in tree peony would be greatly
272 needed.

VIGS technique has been widely used in various plant species as a rapid, convenient, and efficient tool for functional assessment of genes (*Wege et al., 2007*; *Velásquez et al., 2009*). In the present study, whether TRV-based vector could be used for silencing endogenous genes in tree peony was investigated. Our results demonstrated that the conventional leaf syringe-infiltration method is laborious and it resulted in an inadequate infiltration to *P. ostii* leaves, when compared with seedling vacuum-infiltration. It is quite likely that the physiological structure of tree peony leaf affected the entering of agrobacterial mixture. Not many stomatal apparatus existed in the lower epidermis of tree peony young leaf, and its leaf mesophyll cells were divided into a large number of vein islets by reticulate vein networks. Only a limited area of leaf could be effectively infiltrated with TRV constructs via syringe injection. Additionally, the thin tree peony leaves were prone to suffer mechanical damage from syringe-infiltration method. Previous studies also showed that the vacuum approach was more effective than other infiltration methods in woody plants (*Ye et al., 2009*; *Liu et al., 2014*). Thus, a vacuum-infiltration into the whole plant is probably considered as a good choice, when it comes to species that are difficult to infect.

Concerning the experimental materials for inoculation, it is well known that tree peony has a long juvenile stage that commonly lasts for about 3 years, during which the root is the main growing part (*Wang et al., 2015*). This development feature confined the application of VIGS on tree peony plants. Three-year-old seedlings of tree peony were consequently selected as agro-inoculated objects in our work. Since the plants at this stage were favorable to vacuum infiltration in size, and on the other hand to sprouting of upper new leaves. A visual silencing

294 phenotype of marker gene, such as *PDS*-silenced leaf photobleaching or *chalcone synthase* (*CHS*)-
295 silenced white-corollas phenotypes, requires upspring of systemically-infected tissues. Our
296 results proved that a significant gene silencing took place in newly-developed leaves of triennial
297 *P. ostii* plants. Because no reproductive buds were formed at this stage, a trial of gene silencing
298 in tree peony floral organs via VIGS will be made in future work.

299 *PDS* has been frequently used as an indicator gene in VIGS systems because the silencing of
300 *PDS* reduces photoprotective carotenoid levels in green tissues and thereby leads to chlorophyll
301 photooxidation and tissue bleaching (*Kumagai et al., 1995*). In this study, we cloned the *PDS*
302 gene from *P. ostii* leaves and constructed the TRV-*PoPDS* vector to unravel the function of
303 *PoPDS* and verify the possibility of applying VIGS in tree peony. After infiltration with TRV-
304 *PoPDS*, an expected silencing phynotype (photobleaching) was observed in systemically-
305 infected leaves, while the directly inoculated leaves showed lesions resembling those of TRV
306 empty vector. The results mentioned above indicated that a systemic TRV viral infection was
307 established, and it was essential for the VIGS application. The silencing of *PoPDS* also
308 demonstrated that TRV-based VIGS could be used as an effective method towards functional
309 characterization of genes in tree peony plants.

310 It is noteworthy that almost all photobleached leaves resulting from TRV-*PoPDS* infection
311 exhibited variegated phenotypes as white spots or sectors not completely white (Fig. 3a), and we
312 hypothesized that multiple factors may contribute to it. The post-inoculation growth temperature
313 largely influences the efficiency of VIGS-based gene silencing. It has been reported that low
314 temperature enhances gene silencing efficiency when TRV-mediated VIGS is employed in

315 tomato (*Fu et al., 2006*). But a conflicting finding is that low temperature suppresses gene
316 silencing through the prevention of siRNA formation in *N. benthamiana* (*Szittya et al., 2003*).
317 The length of inserted fragment in viral vector is also closely associated with gene silencing
318 efficiency. As reported previously, different lengths of *PDS* inserts result in varied
319 photobleaching patterns and ranges in TRV-infected tobacco (*Liu & Page, 2008*; *Ye et al., 2009*).
320 Our VIGS procedure hence requires further optimization in temperature and inserted fragment
321 size in future work. Furthermore, the *PoPDS*-silenced phenotypes were particularly significant
322 along the leaf vein (Fig. 3a). It is in agreement with the results that viral propagation and/or
323 systemic silencing response occur mainly along the vascular bundle system (*Wege et al., 2007*).

324 In order to visualize viral accumulation in infiltrated tree peony plants, the TRV-GFP vector
325 was used. The GFP, a fluorescent protein from jellyfish (*Aequorea victoria*), does not participate
326 in biological processes of plants. The gene was overexpressed driven by the 35S promoter and
327 used as a marker to trace the presence of virus (*Tian et al., 2014*). In the present work, green
328 fluorescence was observed in the roots and leaves of infected tree peony seedlings at 5 dpi, and
329 the accumulation levels of TRV1, TRV2, and GFP were also detected (Fig. 4). The concentration
330 of GFP protein was able to reflect the viral load and degree of silencing (*Tian et al., 2014*).
331 Previous findings proved that TRV virus possesses the ability to move efficiently within the
332 roots of infected plants (*Macfarlane & Popovich, 2000*). We found a higher transcript and
333 protein levels of GFP in roots than that in leaves. It is concluded that virus infection may happen
334 mainly in roots at first and then spread into newly-developed leaves after vacuum infiltration.
335 Future work will examine the underlying mechanism for the discrepancy of TRV replication and

movement in roots and leaves of tree peony. Altogether, it suggested that the TRV-GFP vector was available to tree peony plants and suitable for monitoring the systemic spread of TRV carrying target gene fragments. An advantage is that the employment of TRV-GFP construct could avoid the destruction of the photosynthetic apparatus caused by *PDS*-silenced leaf photobleaching.

Conclusion

In conclusion, our results indicated that an effective TRV-based VIGS system was established in *P. ostii* based on TRV-*PoPDS* and TRV-GFP constructs. Seedling vacuum-infiltration was determined as an appropriate method for *Agrobacterium*-mediated infection of TRV, compared with leaf syringe-infiltration. A remarkable photobleaching phenotype was observed in TRV-*PoPDS*-infected upper new leaves, which was concomitant with substantial reduction in *PoPDS* transcripts. The detection of GFP fluorescence and accumulation levels in leaves and roots infected with TRV-GFP revealed TRV is a versatile tool to analyze gene function in different tissues of tree peony. Thus, this system we developed will be greatly helpful to characterize the function of genes associated with various molecular and physiological processes in tree peony.

Acknowledgements

We thank Xiang Li and Xiaotong Ji for experimental assistance in agro-infiltration with syringe and vacuum. We are grateful to Yule Liu's favor for kindly providing TRV-GFP vector.

References

Bartel DP. 2004. MicroRNAs: genomics, biogenesis, mechanism, and function. *Cell* **116:**281–297

Baulcombe D. 1999. Viruses and gene silencing in plants. *Arch Virol Suppl* **15:**189–201

Bradford M. 1976. A rapid and sensitive method for quantitation of microgram quantities of protein utilizing the principle of proteindye binding. *Analytical Biochemistry* **72:**248–254

Burch-Smith T, Anderson J, Martin GK, Sp. 2004. Applications and advantages of virus-induced gene silencing for gene function studies in plants. *Plant Journal* **39:**734–746

Burchsmith TM, Schiff M, Liu Y, Dineshkumar SP. 2006. Efficient virus-induced gene silencing in Arabidopsis. *Plant Physiology* **142:**21–27

Cheng F, Li J, and Yu L. 1998. Exportation of Chinese Tree Peonies (Mudan) and their developments in other countries.II.Wild species. *Estuarine Coastal & Shelf Science* **73:**223–235.

Cunningham FX, and Gantt E. 1998. GENES AND ENZYMES OF CAROTENOID BIOSYNTHESIS IN PLANTS. *Annual Review of Plant Biology* **49:**557-583.

Dinesh-Kumar SP, Anandalakshmi R, Marathe R, Schiff M, and Liu Y. 2011. Virus-induced gene silencing. *Methods Mol Biol* **236:**287-294.

Faivrerampant O, Gilroy EM, Hrubikova K, Hein I, Millam S, Loake GJ, Birch PRJ, Taylor MA, and Lacomme C. 2004. Potato Virus X-Induced Gene Silencing in Leaves and Tubers of Potato. *Plant Physiology* **134:**1308-1316.

Fu DQ, Zhu BZ, Zhu HL, Zhang HX, Xie YH, Jiang WB, Zhao XD, and Luo KB. 2006. Enhancement of virus-induced gene silencing in tomato by low temperature and low humidity. *Molecules & Cells* **21:**153-160.

Holzberg S, Brosio P, Gross CS, and Pogue GP. 2002. Barley stripe mosaic virus‐induced gene silencing in a monocot plant. *Plant Journal* **30:**315-327.

Jia HF, Chai YM, Li CL, Lu D, Luo JJ, Qin L, and Shen YY. 2011. Abscisic acid plays an important role in the regulation of strawberry fruit ripening. *Plant Physiology* **157:**188.

Kumagai MH, Donson J, Dellacioppa GR, Harvey D, Hanley KM, and Grill LK. 1995. Cytoplasmic inhibition of carotenoid biosynthesis with virus-derived RNA. *Proceedings of the National Academy of Sciences of the United States of America* **92:**1679-1683.

Kurth EG, Peremyslov VV, Prokhnevsky AI, Kasschau KD, Miller M, Carrington JC, and Dolja VV. 2012. Virus-Derived Gene Expression and RNA Interference Vector for Grapevine. *Journal of Virology* **86:**6002-6009.

Li C, Hui DU, and Wang L. 2009. Flavonoid Composition and Antioxidant Activity of Tree Peony (Paeonia Section Moutan) Yellow Flowers. *Journal of Agricultural & Food Chemistry* **57:**8496-8503.

Li J, Han J, Hu Y, and Yang J. 2016. Selection of Reference Genes for Quantitative Real-Time PCR during Flower Development in Tree Peony (*Paeonia suffruticosa Andr.*). *Front Plant Sci* **7:**516.

Li S, Wu Q, Yin D, Feng C, Liu Z, and Wang L. 2018. Phytochemical variation among the traditional Chinese medicine Mu Dan Pi from Paeonia suffruticosa (tree peony). *Phytochemistry* **146:**16-24.

Liu E, and Page JE. 2008. Optimized cDNA libraries for virus-induced gene silencing (VIGS) using tobacco rattle virus. *Plant Methods* **4:**5-5.

Liu HC, and Jia WQ. 2010. Establishment of plantlet regeneration system of tree peony through lateral buds cutting and carving. *Acta Horticulturae Sinica* **37:**1471-1476.

Liu Y, Schiff M, and Dineshkumar SP. 2002. Virus‐induced gene silencing in tomato. *Plant Journal* **31:**777-786.

Liu Y, Wei S, Zeng S, Huang W, Di L, Hu W, Shen X, and Ying W. 2014. Virus-induced gene silencing in two novel functional plants, Lycium barbarum L. and Lycium ruthenicum Murr. *Scientia Horticulturae* **170:**267-274.

Luo J, Shi Q, Niu L, and Zhang Y. 2017. Transcriptomic Analysis of Leaf in Tree Peony Reveals Differentially Expressed Pigments Genes. *Molecules* **22:**324.

Macfarlane SA, and Popovich AH. 2000. Efficient expression of foreign proteins in roots from tobravirus vectors. *Virology* **267:**29-35.

Purkayastha A, and Dasgupta I. 2009. Virus-induced gene silencing: a versatile tool for discovery of gene functions in plants. *Plant Physiology and Biochemistry* **47:**967-976.

Ratcliff F, ., Martin-Hernandez AM, and Baulcombe DC. 2001. Technical Advance. Tobacco rattle virus as a vector for analysis of gene function by silencing. *Plant Journal* **25:**237–245.

Reid M, Chen JC, and Jiang CZ. 2009. Virus-Induced Gene Silencing for Functional Characterization of Genes in Petunia. In: Gerats T, Strommer J, eds. Petunia. Berlin Heidelberg: Springer, 381–394.

Robertson NL, Brown KL, Winton LM, and Holloway PS. 2009. First report of Tobacco rattle virus in Peony in Alaska. Plant Disease **93:**675-675.

Ruiz MT, Voinnet O, and Baulcombe DC. 1998. Initiation and Maintenance of Virus-Induced Gene Silencing. *The Plant Cell* **10:**937-946.

Senthilkumar M, and Mysore KS. 2011. New dimensions for VIGS in plant functional genomics. *Trends in Plant Science* **16:**656-665.

Singh A, Kumar P, Jiang CZ, and Reid MS. 2013. TRV Based Virus Induced Gene Silencing in Gladiolus (Gladiolus grandiflorus L.), A Monocotyledonous Ornamental Plant. *International Journal of Plant Research* **26:**170.

Stilio VS, Di, Kumar RA, Oddone AM, Tolkin TR, Patricia S, and Kacie MC. 2010. Virus-induced gene silencing as a tool for comparative functional studies in Thalictrum. *Plos One* 5:e12064.

Sun D, Li S, Niu L, Reid MS, Zhang Y, and Jiang C. 2017. PhOBF1, a petunia ocs element binding factor, plays an important role in antiviral RNA silencing. *Journal of Experimental Botany* **68:**915-930.

Sun D, Nandety RS, Zhang Y, Reid MS, Niu L, and Jiang C. 2016. A petunia ethylene-responsive element binding factor, PhERF2, plays an important role in antiviral RNA silencing. *Journal of Experimental Botany* **67:**3353-3365.

Szittya G, Silhavy D, Molnar A, Havelda Z, Lovas A, Lakatos L, Banfalvi Z, and Burgyan J. 2003. Low temperature inhibits RNA silencing-mediated defence by the control of siRNA generation. *The EMBO Journal* **22:**633-640.

Tasaki K, Terada H, Masuta C, and Yamagishi M. 2016. Virus-induced gene silencing (VIGS) in Lilium leichtlinii using the Cucumber mosaic virus vector. *Plant Biotechnology* **33:**373-381.

Tian J, Pei H, Zhang S, Chen J, Chen W, Yang R, Meng Y, You J, Gao J, and Ma N. 2014. TRV–GFP: a modified Tobacco rattle virus vector for efficient and visualizable analysis of gene function. *Journal of Experimental Botany* **65:**311-322.

Velásquez AC, Chakravarthy S, and Martin GB. 2009. Virus-induced gene silencing (VIGS) in Nicotiana benthamiana and tomato. *Journal of Visualized Experiments* **28:** 1292.

Wang S, Beruto M, Xue J, Zhu F, Liu C, Yan Y, and Zhang X. 2015. Molecular cloning and potential function prediction of homologous SOC1 genes in tree peony. *Plant Cell Reports* **34:**1459-1471.

Wege S, Scholz A, Gleissberg S, and Becker A. 2007. Highly Efficient Virus-induced Gene Silencing (VIGS) in California Poppy (Eschscholzia californica): An Evaluation of VIGS as a Strategy to Obtain Functional Data from Non-model Plants. *Annals of Botany* **100:**641-649.

Wu J, Cai C, Cheng F, Cui H, and Zhou H. 2014. Characterisation and development of EST-SSR markers in tree peony using transcriptome sequences. *Molecular Breeding* **34:**1853-1866.

Wu L, Ma N, Jia Y, Zhang Y, Feng M, Jiang CZ, Ma C, and Gao J. 2016. An ethylene-induced regulatory module delays flower senescence by regulating cytokinin content. *Plant Physiology* **173**: 853-862.

Yamagishi N, and Yoshikawa N. 2013. Highly Efficient Virus-Induced Gene Silencing in Apple and Soybean by Apple Latent Spherical Virus Vector and Biolistic Inoculation. *Methods of Molecular Biology* **975**:167-181.

Yan H, Fu D, Zhu B, Liu H, Shen X, and Luo Y. 2012. Sprout vacuum-infiltration: a simple and efficient agroinoculation method for virus-induced gene silencing in diverse solanaceous species. *Plant Cell Reports* **31**:1713-1722.

Ye J, Qu J, Bui HTN, and Chua N. 2009. Rapid analysis of Jatropha curcas gene functions by virus‐induced gene silencing. *Plant Biotechnology Journal* **7**:964-976.

Yin DD, Xu WZ, Shu QY, Li SS, Wu Q, Feng CY, Gu ZY, and Wang LS. 2018. Fatty acid desaturase 3 (PsFAD3) from Paeonia suffruticosa reveals high α -linolenic acid accumulation. *Plant Science* **274**:212-222.

Zhang J, Yu D, Zhang Y, Liu K, Xu K, Zhang F, Wang J, Tan G, Nie X, and Ji Q. 2017. Vacuum and Co-cultivation Agroinfiltration of (Germinated) Seeds Results in Tobacco

474 Rattle Virus (TRV) Mediated Whole-Plant Virus-Induced Gene Silencing (VIGS) in Wheat
475 and Maize. *Frontiers in Plant Science* **8:**393.
476 **Zhang Q, Yu R, Xie L, Rahman M, Kilaru A, Niu L, and Zhang Y. 2018.** Fatty Acid and
477 Associated Gene Expression Analyses of Three Tree Peony Species Reveal Key Genes for
478 α-Linolenic Acid Synthesis in Seeds. *Frontiers in Plant Science* **9:**106.
479 **Zhang Y, Cheng Y, Ya H, Xu S, and Han J. 2015a.** Transcriptome sequencing of purple petal
480 spot region in tree peony reveals differentially expressed anthocyanin structural genes.
481 *Frontiers in Plant Science* **6:**964.
482 **Zhang Y, Zhang L, Gai S, Liu C, and Lu S. 2015b.** Cloning and expression analysis of the
483 R2R3-PsMYB1 gene associated with bud dormancy during chilling treatment in the tree
484 peony (Paeonia suffruticosa). *Plant Growth Regulation* **75**:667-676.

Table 1(on next page)

Primers used for RT-PCR amplification and construction of recombinant TRV2 plasmids

Table 1 Primers used for RT-PCR amplification and construction of recombinant TRV2 plasmids.

Primer name	Nucleotide sequence (5'-3')	Purpose	Size
PoPDS-F1	TCGGAGTTGGGTTCGCTGC	Cloning of *PoPDS* coding region	1797bp
PoPDS-R1	ATTCTGATGTGTTTTGTAGCC		
PoPDS-F2	CAGCCGATTTGATTTCCTTG	Cloning of inserted fragment for VIGS	195bp
PoPDS-R2	CCTTGTTTTCTCATCCAGTC		
PoPDS-F3	AGTCATTGGGGGGTCAGGTCCG	RT-PCR	312bp
PoPDS-R3	CAGCATACACACTCAGAAGGGG		
TRV1-F	CAGTCTATACACAGAAACAGA	TRV1-RNA detection	463bp
TRV1-R	GACGTGTGTACTCAAGGGTT		
TRV2-1F	GGCTAACAGTGCTCTTGGTG	TRV2-RNA detection	359bp
TRV2-1R	GTATCGGACCTCCACTCGC		
TRV2-2F	CGAGTGGAGGTCCGATACG	TRV2-RNA (containing inserted fragment) detection	Depending on insert
TRV2-2R	CGGTTCATGGATTCGGTTAG		
GFP-F	ATGGCCAACACTTGTCACTACTT	GFP-RNA detection	260bp
GFP-R	ATTCCAATTTGTGTCCAAGAATG		
18S-26S-ITS-F	ACCGTTGATTCGCACAATTGGTCA	RT-PCR	150bp
18S-26S-ITS-R	TACTGCGGGTCGGCAATCGGACG		

Figure 1

Comparison of syringe-infiltration and vacuum-infiltration methods with the TRV empty vector

a Three-year-old *P. ostii* plantlets at 4 weeks post germination used for agro-infiltration. **b** Schematic depiction of *Agrobacterium*-mediated TRV inoculation in *P. ostii* plants using syringe and vacuum methods. **c** The *P. ostii* leaves subjected to syringe- and vacuum-infiltration with TRV empty vector. **d** Semi-quantitative RT-PCR analysis of TRV1 and TRV2-1 accumulation levels in TRV empty vector-inoculated leaves by syringe and vacuum methods. 18S-26S internal transcribed spacer (18S-26S ITS) was used as internal standard.

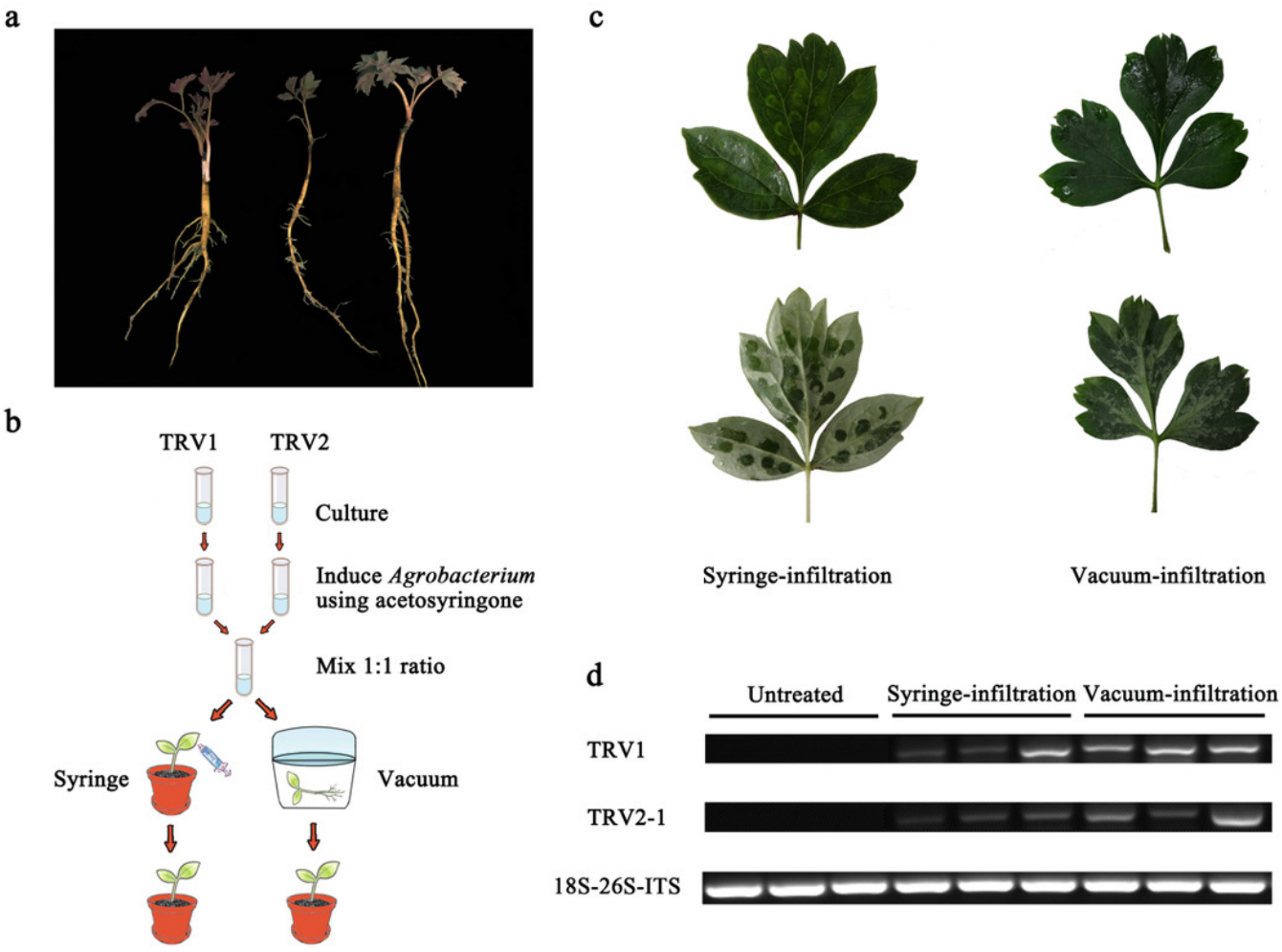

Figure 2

Schematic representation of TRV constructs used in this study

a The cDNA of *PoPDS* insert for its introduction into TRV vector. PoPDS-F1/PoPDS-R1 was used to amplify the open reading frame region of *PoPDS*, PoPDS-F2/PoPDS-R2 targeted the inserted fragment of *PoPDS* (the black box), and PoPDS-F3/PoPDS-R3 was designed for quantitative real-time PCR. **b** The structures of TRV1, TRV2, TRV2-*PoPDS*, and TRV2-GFP. The arrows indicate the different primer pairs for examining TRV1, TRV2-1, TRV2-2, and GFP transcript levels. LB left border, RB right border, MP movement protein, 16K 16 Kd protein, Rz self-cleaving ribozyme, NOSt NOS terminator, CP coat protein, MCS multiple cloning site.

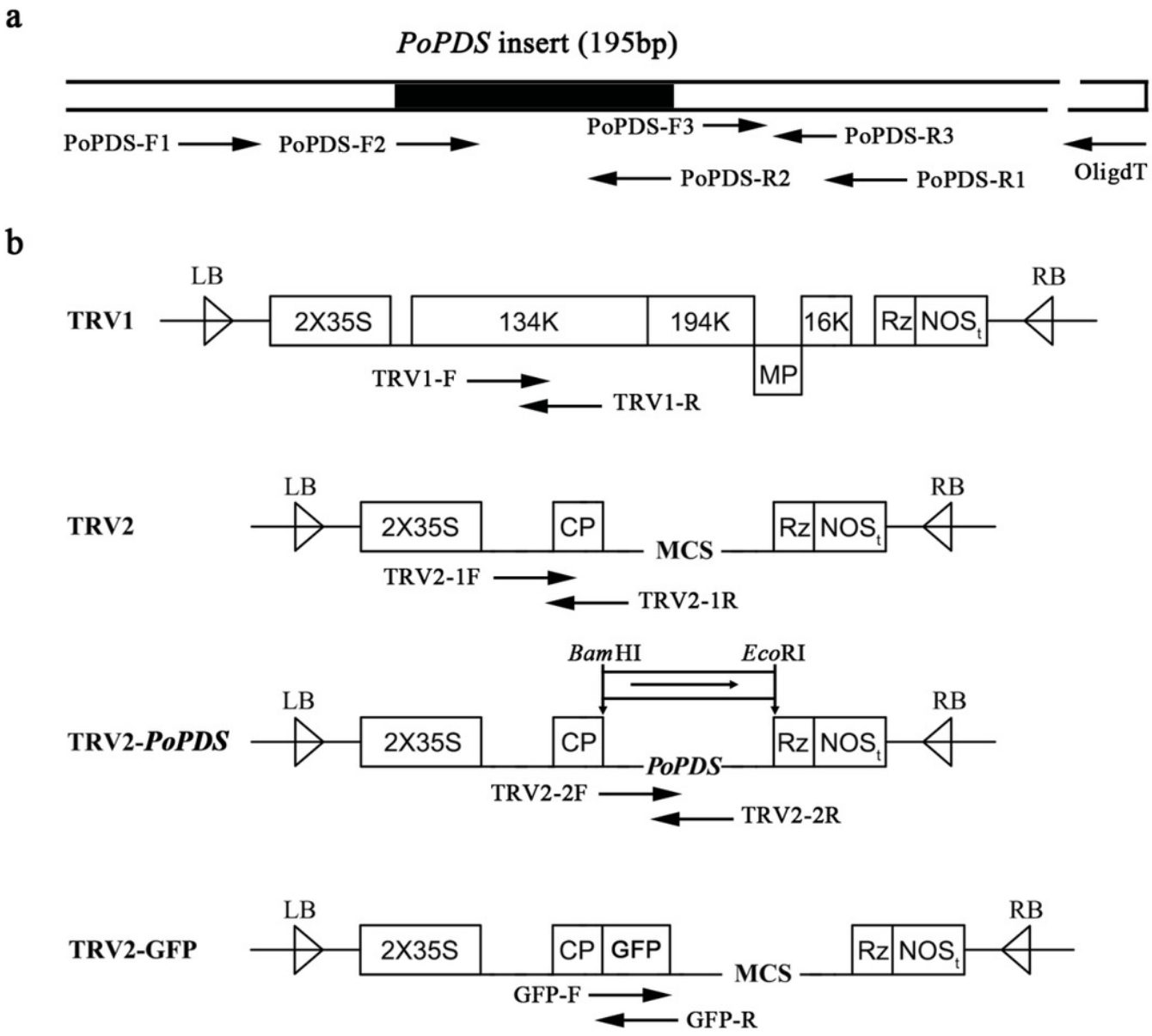
a
PoPDS insert (195bp)
PoPDS-F1
PoPDS-F2
PoPDS-F3
PoPDS-R3
PoPDS-R2
PoPDS-R1
OligdT
b
TRV1
LB
2X35S
134K
194K
16K
MP
Rz
NOS
RB
TRV1-F
TRV1-R
TRV2
CP
MCS
TRV2-1F
TRV2-1R
TRV2-PoPDS
BamHI
EcoRI
PoPDS
TRV2-2F
TRV2-2R
TRV2-GFP
GFP
GFP-F
GFP-R

Figure 3

Silencing of *PoPDS* in *P. ostii* leaves infected with TRV-*PoPDS*

a Representative phenotypes of mock treated, TRV- (empty vector), and TRV-*PoPDS*-infected leaves in *P. ostii* seedlings. Photobleaching phenotypes were observed in the first newly-developed leaves of seedlings at 5 weeks post infiltration with TRV-*PoPDS*. **b** Semi-quantitative RT-PCR analysis of TRV1 and TRV2 accumulation levels in agro-infected *P. ostii* leaves.**c** Quantitative real-time PCR analysis of *PoPDS* in agro-infected *P. ostii* leaves. 18S-26S internal transcribed spacer (18S-26S ITS) was used to normalize the transcript levels, and relative expression values were calculated compared with the highest expression value taken as 1.0 (untreated). Error bars represent ±SE of data from three independent experiments. The different letters indicate significant differences using Duncan's multiple range test at $p<0.05$.

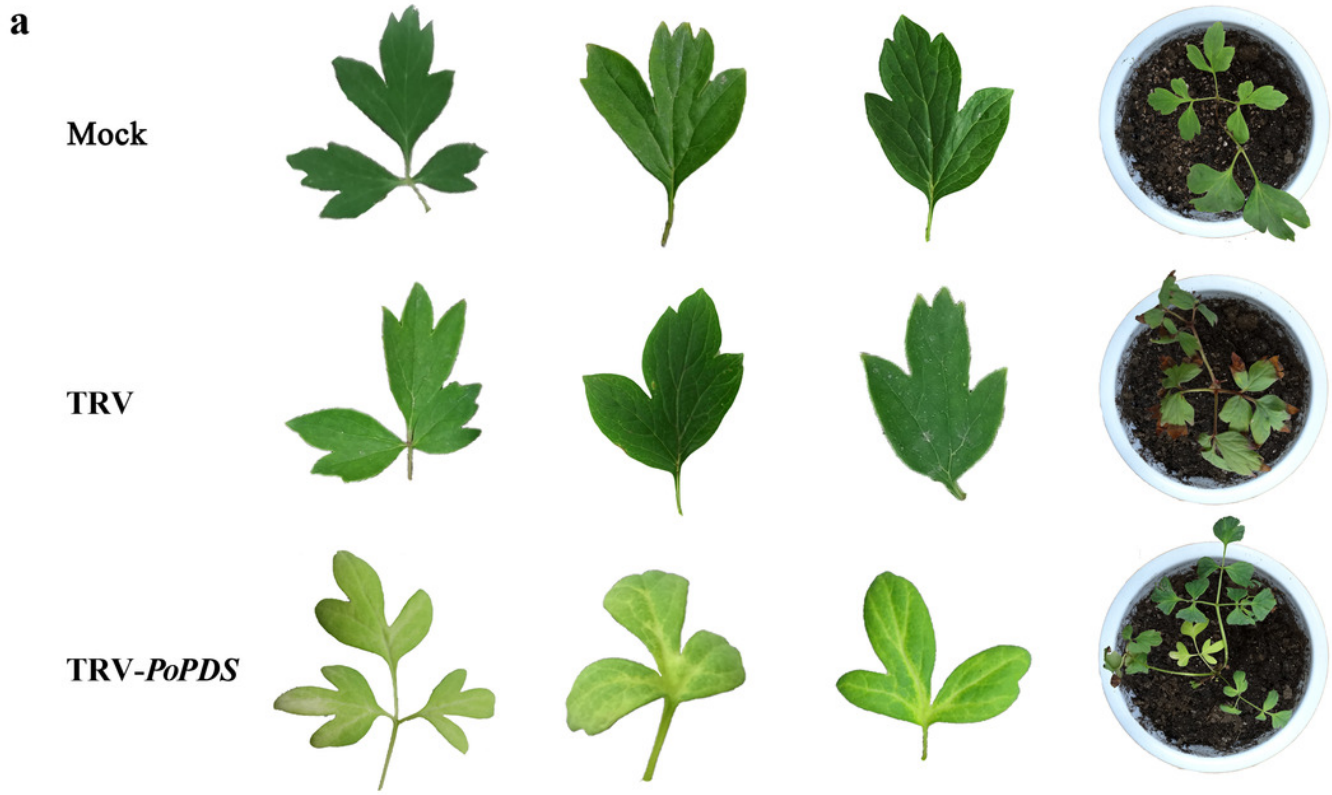
a
Mock
TRV
TRV-PoPDS
b
Mock
TRV
TRV-PoPDS
TRV1
TRV2-1
TRV2-2
18S-26S-ITS
c
Relative PoPDS expression
1.2
0.8
0.4
0
a
a
b
Mock
TRV
TRV-PoPDS

Figure 4

GFP expression in *P. ostii* leaves and roots inoculated with TRV-GFP

Confocal microscopy image of P. ostii leaves and roots infected with TRV-GFP at 5 days post-infiltration (dpi). Fluorescence was not observed in leaves (a-c) and roots (g-i) of mock-treated plants. The bright field (a, d, g, j), the GFP channel (b, e, h, k), and the merged images (c, f, i, l) of the bright field and the GFP channel are shown. Scale bars equal to 100 μm (a-f) or 75 μm (g-l).

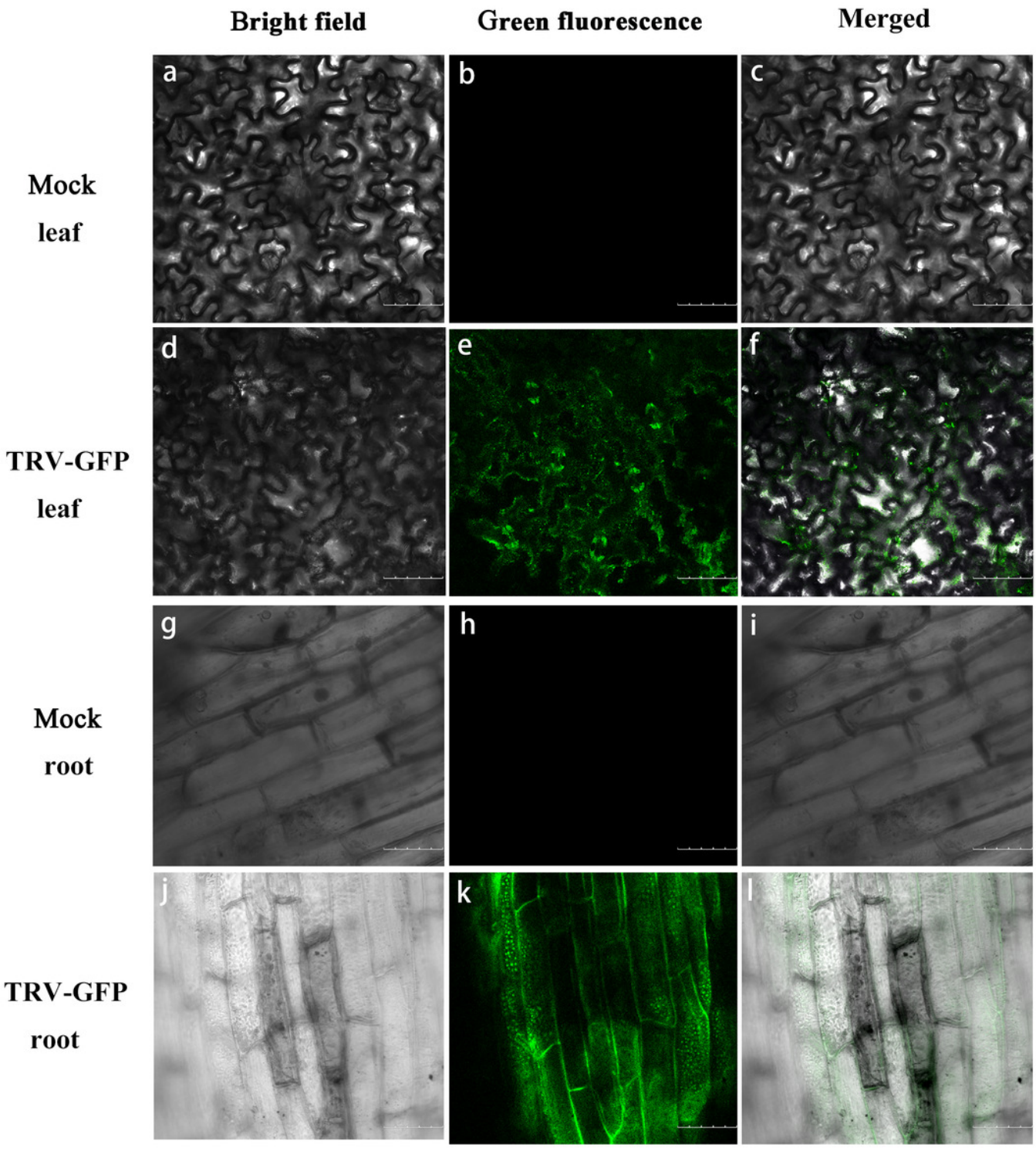
Bright field
Green fluorescence
Merged
Mock leaf
TRV-GFP leaf
Mock root
TRV-GFP root
a
b
c
d
e
f
g
h
i
j
k
l

Figure 5

Detection of GFP protein accumulation in TRV-GFP-inoculated *P. ostii* leaves and roots

a Western blot analysis of CP-GFP protein levels in mock treated, TRV-GFP-infected *P. ostii* leaves and roots at 5 days post inoculation. Ten micrograms of protein were loaded into each lane and an anti-GFP antibody was used to detect the CP-GFP fusion protein. Coomassie blue staining was used to confirm equal loading in each lane. **b** Semi-quantitative RT-PCR analysis of TRV1, TRV2, and GFP accumulation levels in mock treated, TRV-GFP-infected *P. ostii* leaves and roots. 18S-26S internal transcribed spacer (18S-26S-ITS) was used as internal control.

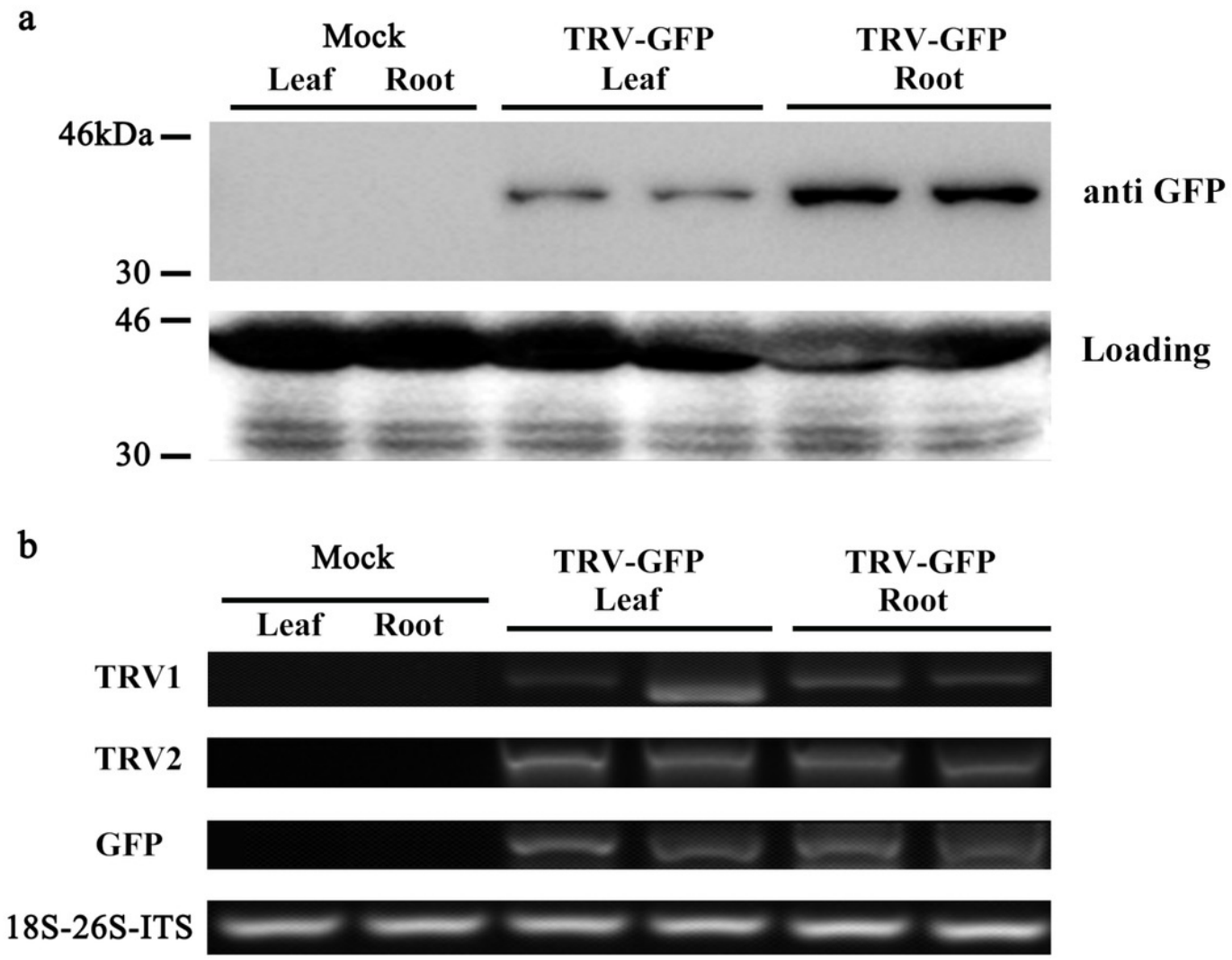
a
Mock
Leaf
Root
TRV-GFP
Leaf
TRV-GFP
Root
46kDa
30
46
30
anti GFP
Loading
b
Mock
Leaf
Root
TRV-GFP
Leaf
TRV-GFP
Root
TRV1
TRV2
GFP
18S-26S-ITS